Supplementary methods

Baumdick and Niehrs et al.

HLA-DP on Epithelial Cells enables Tissue Damage by NKp44+ Cells in Ulcerative Colitis

Imputation & Phasing with the Michigan Imputation Server

Imputation was performed on the Michigan Imputation Server with a multi-ethnic reference panel (version 1.0 2021; full context HLA panel) published by[1] that contained 18,293 individuals and 54,474 sites including amino acid, SNP and *HLA* allele information. Results were received as a single VCF-File with genotype, genotype dosage and genotype probability as well as genotype phase information given for each individual and *HLA* allele. Using the given phase information, alleles were combined into *HLA-DPA1-DPB1* haplotypes at 2-field level based on VCF-file genotype hardcalls using PLINK version 1.9[2] and R version 3.6.2. Individuals with missing allele information after imposing the above frequency and imputation quality cut-offs, were set to missing for both parental haplotypes. This left in total 13,717 UC cases and 26,417 controls for analysis. In total 3 2-field HLA-*DPA1* and 19 2-field HLA-*DPB1* alleles were imputed into the data with an allele frequency > 0.5%. All had an imputation score (R^2) > 0.6.

Imputation & Phasing with HLA genotype Imputation with Attribute Bagging (HIBAG)

Imputation and phasing were performed as described in detail in a previous publication.[3,4] In brief, *HLA* alleles were imputed for *HLA-DPA1*, *-DPB1* using HIBAG and multi-ethnic reference panel, containing 1,300 individuals at 2-digit full HLA context. Phasing was performed by comparison of SNP haplotypes from 10 random out of 100 HIBAG classifiers stored in the HIBAG reference model and SNP haplotypes phased using SHAPEIT2. Phasing certainty was determined as the number of congruent phasing results across 10 of the 100 random classifiers. Individuals with HLA genotype imputation quality scores above 0.8 for *HLA-DPA1* or *HLA-DPB1* and a per locus phasing certainty above 0.6 were included in the analysis. This left in total 13,134 UC cases and 25,248 controls. In total 4 2-field *HLA-DPA1* and 15 2-field

HLA-DPB1 alleles were imputed into the data with allele frequency > 0.5%. Of these all had an imputation (marginal probability as calculated in [5]) score > 0.6.

(Online) Results of HLA-haplotype analysis

The overall correlation between allele frequencies imputed into the data across the imputation with HIBAG and the Michigan Imputation Server was high with a Pearson correlation coefficient of 0.997. Alleles with strikingly deviating allele frequencies included *DPB1*06:01*, which had an allele frequency of 1.7% in the data imputed with the Michigan Imputation Server and of < 0.5% in the data imputed with HIBAG. This allele had previously been associated with UC.[6] Here we could not replicate this association (*P* = 0.09, OR=0.904, OR_95L=0.804, OR_95U=1.017), although the genotype data used were nearly identical. In comparison to the imputation score of 0.5 for this allele described previously,[6] we achieved a higher imputation accuracy score of 0.85 with the multi-ethnic panel,[1] which may explain this discrepancy. In addition, we observed deviating frequencies for *HLA-DPA1*01:03* and *HLA-DPA1*02:01* and haplotypes thereof. We observed during phasing with HIBAG that particularly *DPA1*01:03* and *DPA1*02:01* were challenging to phase, both alleles being at instances assigned the same phase if they occurred in the same individual. While *DPA1*01:03* had frequencies of 87.1% (imputation score=1.00) and 82.5% (R^2=0.96) in the data imputed with HIBAG and the Michigan Imputation Server respectively, *DPA1*02:01* had frequencies of a 10.5% (imputation score=0.94) and 13.9% (R^2=0.99). Since both imputation accuracies are high with HIBAG and the Michigan Imputation Server, association analyses on HLA typed *DPA1*01:03/DPA1*02:01* should be analysed in more detail in future studies. This is also true for reanalysis of the association of *HLA-DPB1*06:01* with UC.

Supplementary Table 2: qPCR primer sequences

GAPDH	fwd	CGGAGTCAACGGATTTGG
GAPDH	rev	TGATGACAAGCTTCCCGTTC
IFNg	fwd	ACTGACTTGAATGTCCAACGCA
IFNg	rev	ATCTGACTCCTTTTTCGCTTCC
TNF	fwd	CTCTTCTGCCTGCTGCTGCACTTTG
TNF	rev	ATGGGCTACAGGCTTGTCACTC

Supplementary Table 3: EM for intestinal organoid culture

	Final concentration	company	catalogue number
AD+++	17,5% (v/v)		
B27 supplement	1x	Thermo Fisher	17504001
N2 supplement	1x	Thermo Fisher	17502001
murine EGF	50 ng/ml	Pepro-Tech	315-09-500
N-acetyl-L-cysteine	1.25 mM	Sigma-Aldrich	A9165-25G
[Leu15]-Gastrin	10 nM	Sigma-Aldrich	G9145-.1MG
Nicotinamide	10 mM	Sigma-Aldrich	N0636-100G
SB202190	10 μM	Sigma-Aldrich	S7067-25MG
A83-01	500 nM	Tocris	2939/10
Noggin-CM	10% (v/v)	home-made	
R-spondin-1-CM	20% (v/v)	home-made	
WNT3a-CM	50% (v/v)	home-made	

Supplementary Table 4: Results of the HLA-DPA1-DPB1 haplotype analysis.

See excel file.

Supplementary Table 5: Summary of UC risk and protective alleles of HLA-DR and -DQ.

See excel file.

References

1. Luo, Y. *et al.* A high-resolution HLA reference panel capturing global population diversity enables multi-ancestry fine-mapping in HIV host response. *Nat. Genet.* **53**, (2021).
2. Purcell, S. *et al.* PLINK: A tool set for whole-genome association and population-based linkage analyses. *Am. J. Hum. Genet.* **81**, (2007).
3. Zheng, X. *et al.* HIBAG - HLA genotype imputation with attribute bagging. *Pharmacogenomics J.* **14**, (2014).
4. Degenhardt, F. *et al.* Construction and benchmarking of a multi-ethnic reference panel for the imputation of HLA class I and II alleles. *Hum. Mol. Genet.* **28**, (2019).
5. Degenhardt, F. *et al.* Transethnic analysis of the human leukocyte antigen region for ulcerative colitis reveals not only shared but also ethnicity-specific disease associations. *Hum. Mol. Genet.* **30**, (2021).
6. Goyette, P. *et al.* High-density mapping of the MHC identifies a shared role for HLA-DRB1∗01:03 in inflammatory bowel diseases and heterozygous advantage in ulcerative colitis. *Nat. Genet.* **47**, (2015).

Supplementary figures

Baumdick and Niehrs et al.

HLA-DP on Epithelial Cells enables Tissue Damage by NKp44+ Cells in Ulcerative Colitis

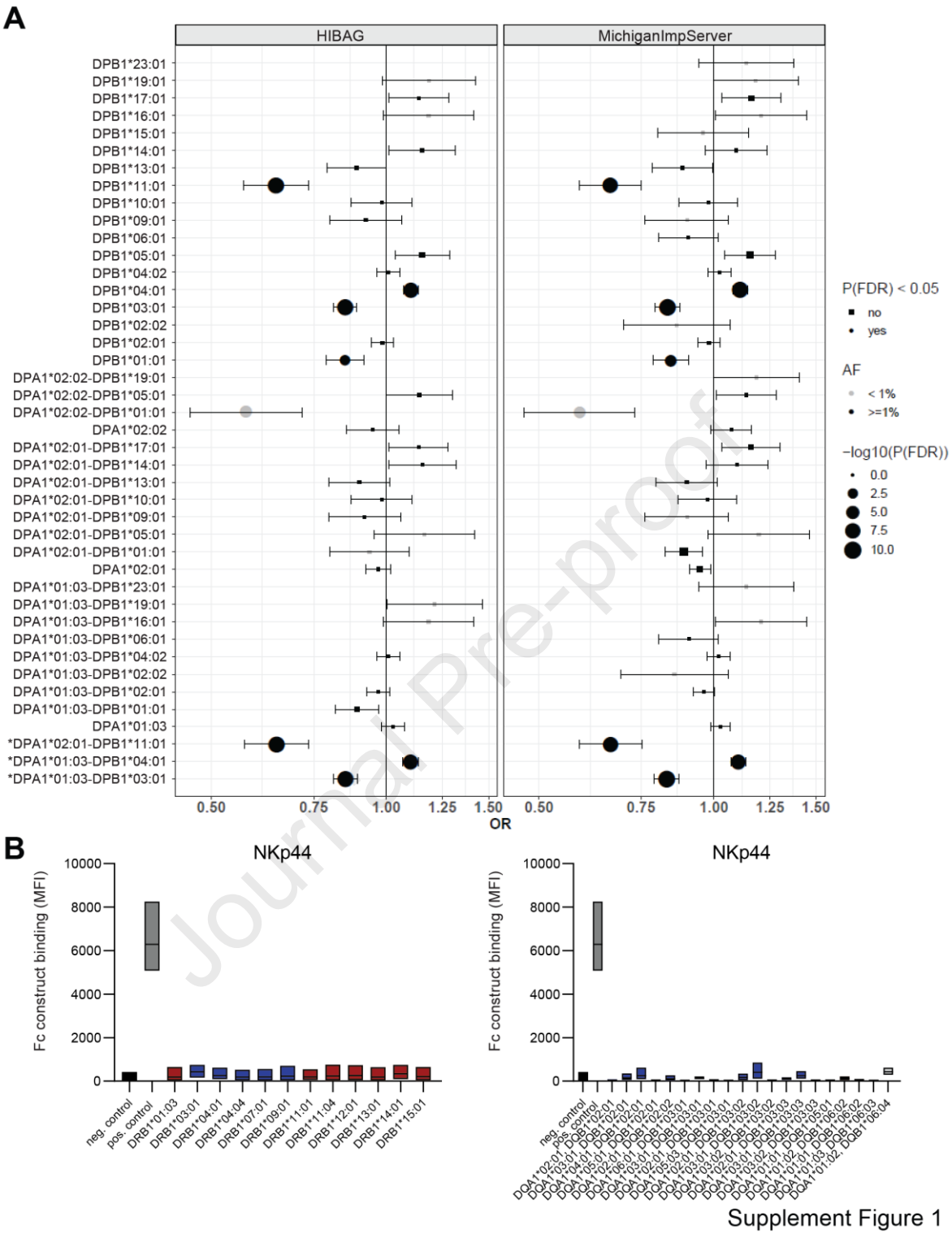

Supplement Figure 1

Supplementary Figure 1: Associations of HLA-DPA1 and HLA-DPB1 alleles and HLA-DPA1-DPB1 haplotypes with UC. A. Imputation of HLA-DPA1-DPB1 haplotypes using HIBAG and MichiganImpServer showing UC risk and protective HLA-DPA1/DPB1 alleles and HLA-DPA1-DPB1 haplotypes with their frequencies and False Discovery Rate *P*-values (P(FDR)). Odds ratios (OR) and 95% confidence intervals (95%CI) are indicated. **B.** NKp44

Fc construct binding to beads coated with different HLA-DR (left panel) or HLA-DQ molecules (right panel) was determined and medians of fluorescence intensity (MFIs) are depicted (n= 6). UC associated risk haplotypes are in red, protective haplotypes are in blue, haplotype combinations of a risk and a protective allele are in light grey. Boxes indicate medians with 25% and 75% quartile ranges, and whiskers indicate minimum and maximum MFI of each HLA-DR/DQ molecule tested.

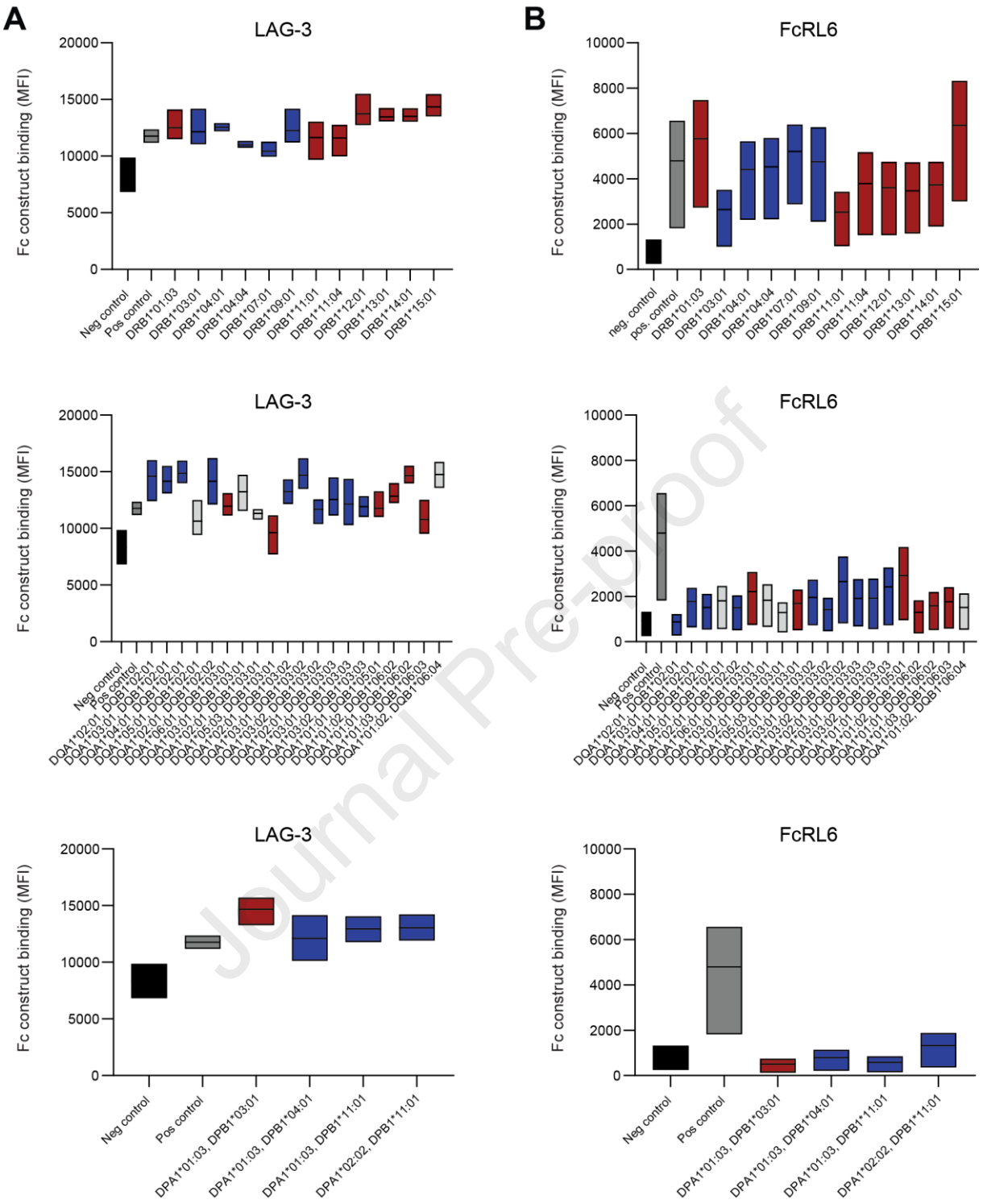

Supplement Figure 2

Supplementary Figure 2: HLA-DR, -DQ and -DP binding to LAG-3 and FcRL6. A. and B. LAG-3 Fc construct (**A**) and FcRL6 Fc construct (**B**) binding to beads coated with different HLA-DR (upper panel), HLA-DQ (middle panel) or HLA-DP molecules (lower panel) were determined and medians of fluorescence intensity (MFIs) are depicted (n= 3). UC associated

risk haplotypes are in red, protective haplotypes are in blue, haplotype combinations of a risk and a protective allele are in light grey. Boxes indicate medians with 25% and 75% quartile ranges, and whiskers indicate minimum and maximum MFI of each HLA-DR/DQ molecule tested.

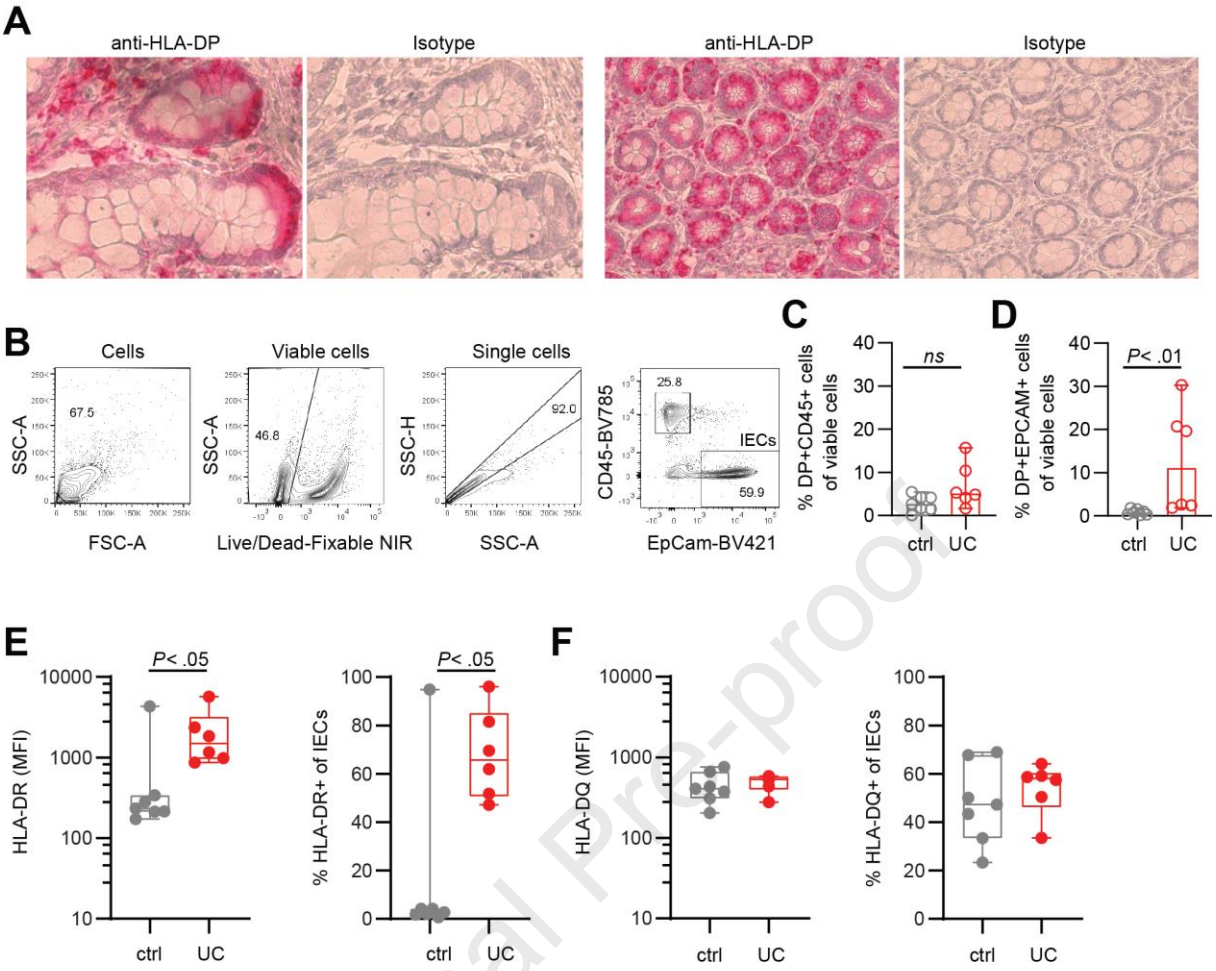

Supplement Figure 3

Supplementary Figure 3: HLA class II upregulation in IECs of individuals with UC. A. Control images of immunohistochemical analyses of UC colon samples. Specific HLA-DP expression is labelled in red, hemalumn was used as a nuclear counterstain (blue). Isotype antibody staining was used as a negative control. **B.** Gating strategy to identify IECs (viable $CD45^{-}EpCam^{+}$) derived from intestinal tissue samples. **C. and D.** Median percentages and

interquartile ranges of HLA-DP$^+$ CD45$^+$ cells (**C**) or HLA-DP$^+$ EpCAM$^+$ IECs (**D**) of all viable cells from controls (n = 7) and UC patients (n = 6) (right panel). **E.** Expression of HLA-DR on EpCam$^+$ IECs depicted as MFI (left panel). Median percentages of HLA-DR$^+$ cells of EpCam$^+$ IECs of controls (n = 7) and UC patients (n = 6) (right panel). **F.** Expression of HLA-DQ on EpCam$^+$ IECs depicted as MFI (left panel). Median percentages of HLA-DQ$^+$ cells of EpCam$^+$ IECs of controls (n = 7) and UC patients (n = 6) (right panel). In **E** and **F**, boxes indicate medians with 25% and 75% quartile ranges, and whiskers indicate minimum and maximum values. Statistical significance was measured using Mann-Whitney U comparisons.

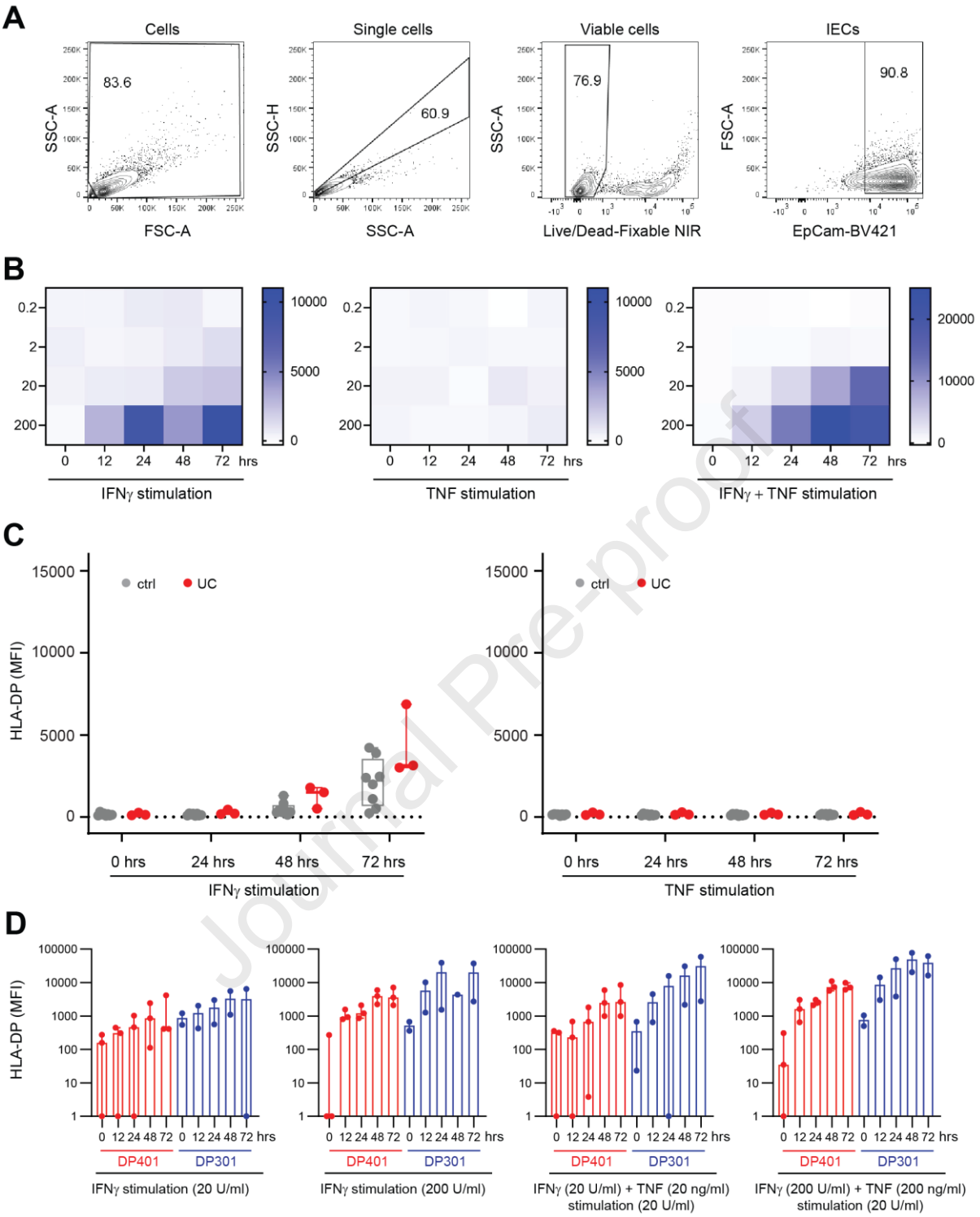

Supplement Figure 4

Supplementary Figure 4: IFNγ- and TNF-mediated upregulation of HLA class II in intestinal organoids. A. Gating strategy to identify (viable EpCam$^+$) IECs derived from intestinal organoids. **B.** Heatmaps showing the MFI of HLA-DP on EpCam$^+$ IECs derived from intestinal organoids upon stimulation with increasing concentrations of IFNγ (U/ml) or TNF

(ng/ml) for the indicated time points (n = 5 donors). **C.** Plots showing MFI of HLA-DP of IECs of control (n = 8) and UC (n = 3) derived intestinal organoids upon IFNγ (100 U/ml, left panel) or TNF stimulation (20 ng/ml, right panel) for the indicated time points. **D.** Plots showing HLA-DP expression of HLA-DP401^{+} (n = 3) and HLA-DP301^{+} (n = 2) IECs derived intestinal organoids upon IFNγ (20 U/ml and 200 U/ml) or stimulation with IFNγ and TNF (IFNγ: 20 U/ml, TNF: 20 ng/ml or IFNγ: 200 U/ml, TNF: 200 ng/ml) for the indicated time points depicted as MFI.

In **C**, boxes indicate medians with 25% and 75% quartile ranges, and whiskers indicate minimum and maximum values. Statistical significance was measured using Mann-Whitney U comparisons.

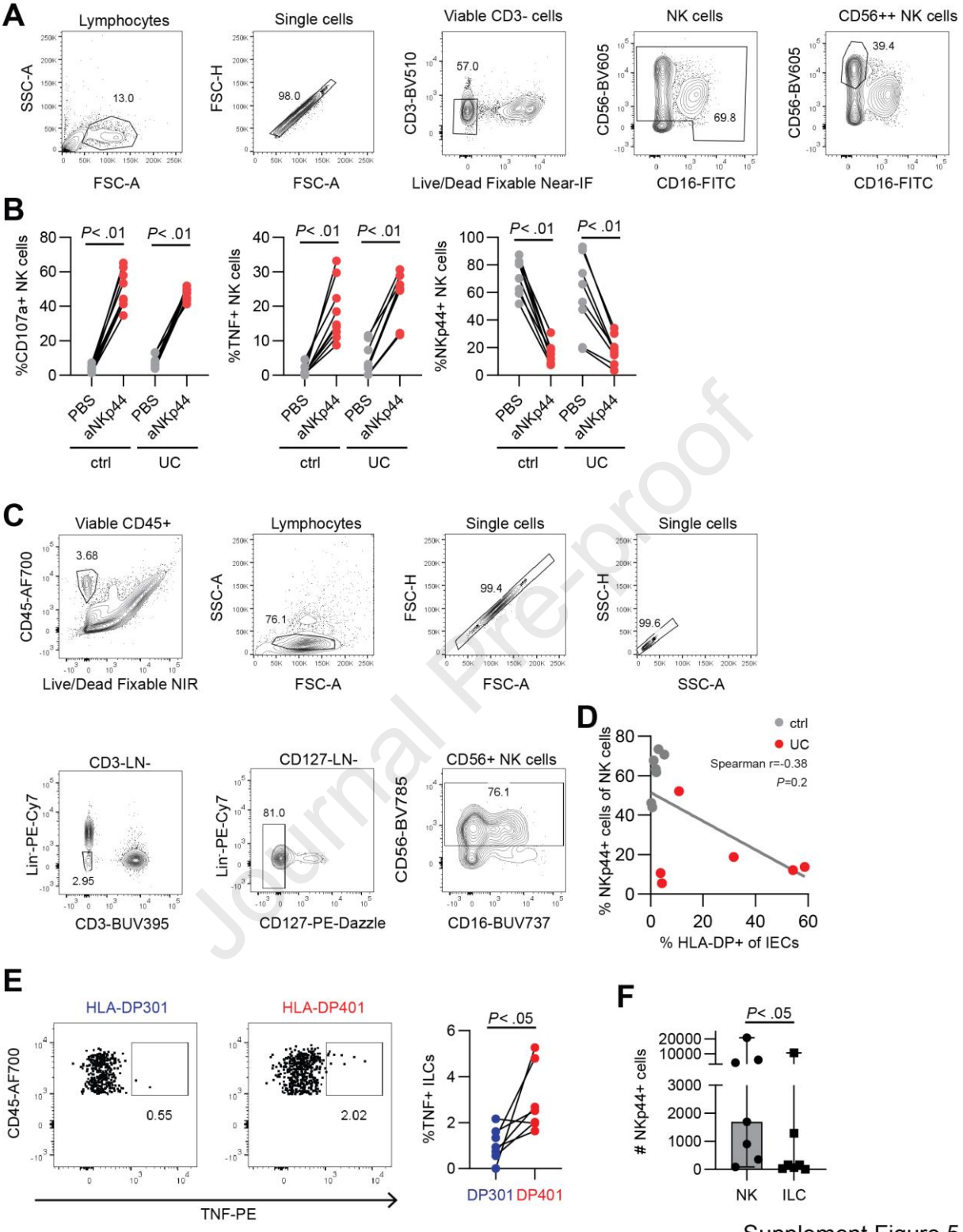

Supplement Figure 5

Supplementary Figure 5: Functional responses of NKp44^{+} NK cells and ILCs after ligand engagement. A. Gating strategy to identify peripheral blood derived CD56^{++} NK cells. **B.** Percentage of CD107a^{+}, TNF^{+} or NKp44^{+} NK cells are shown for control (PBS) and paired stimulated (anti-NKp44) CD56^{++} NK cells (ctrl: n = 9 replicates of 5 donors; UC: n = 8 replicates

of 4 donors). **C.** Gating strategy for intestinal NK cells. NK cells are defined as viable $CD45^+$, $lineage^-$ (Lin^-:$CD14^-$, $CD19^-$, $BDCA2^-$, $CD1a^-$, $CD123^-$, $CD34^-$), $CD3^-$, $CD127^-$ and $CD56^+$ cells. **D.** Plot showing correlation between percentages of HLA-DP^+ IECs and $NKp44^+$ NK cells of the same donor (ctrl and UC; n = 13). Line indicates linear regression. **E.** Representative flow cytometric plots showing TNF expression of intestinal ILCs after stimulation with HLA-DP301 or HLA-DP401 molecules (left panel). Plot shows percentages of TNF^+ ILCs (right panel) (n = 7 donors). **F.** Median counts and interquartile ranges of epithelial $NKp44^+$ NK cells and $NKp44^+$ ILCs per cm^2 (n = 7).

Statistical significance was measured using Wilcoxon-signed rank (**B**, **E**) or Mann-Whitney U comparisons (**F**).

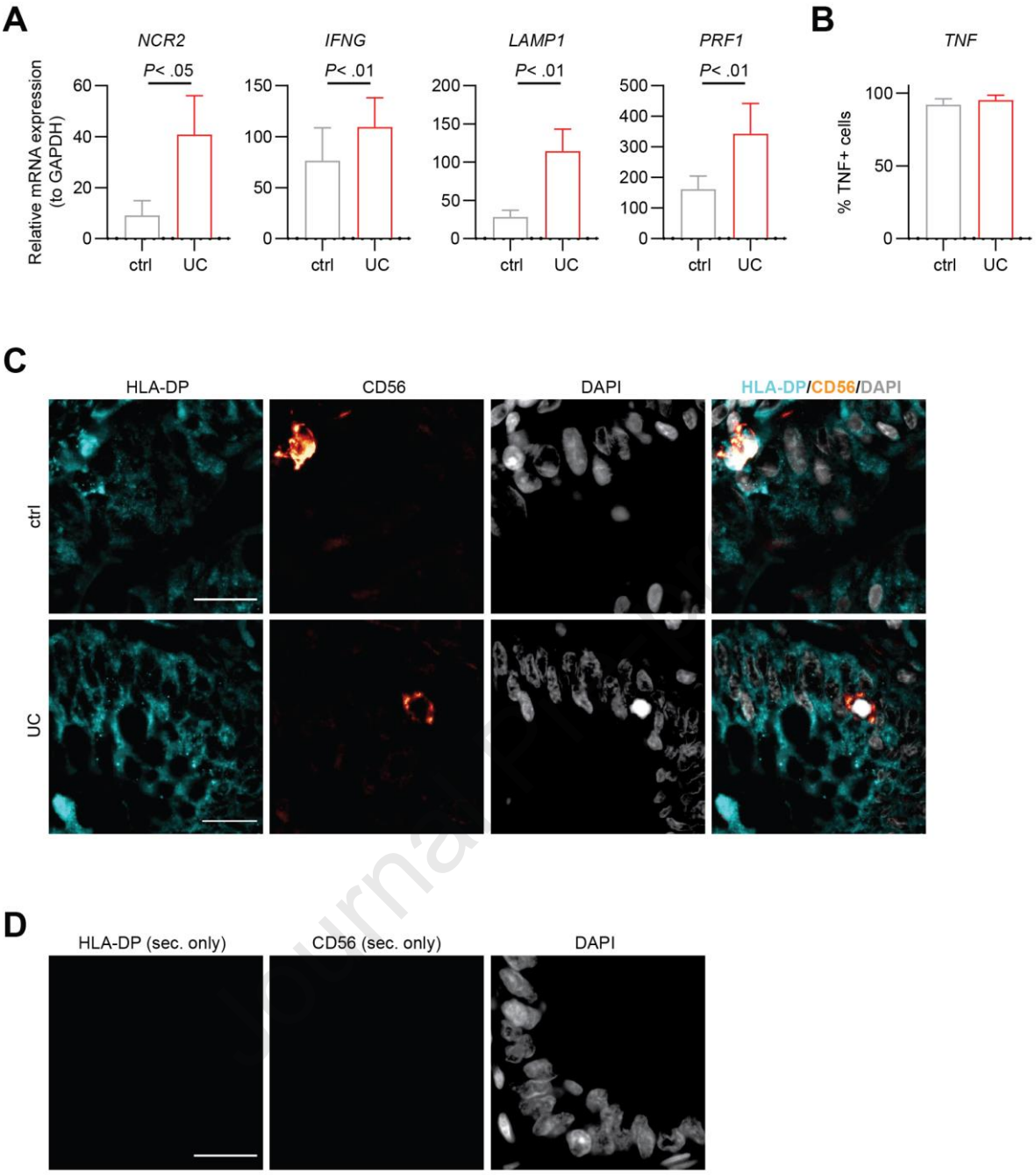

Supplement Figure 6

Supplementary Figure 6: Gene expression of NK cells in intestinal epithelium of individuals with UC and controls. A. Plots showing mean + SEM of relative mRNA expression of *NCR2* (encoding NKp44), *IFNG*, *LAMP1* (encoding CD107a) and *PRF1* (encoding perforin) to reference gene *GAPDH* of single NK cells of controls (n = 80 cells of 3

donors) or individuals with UC (n = 86 cells of 3 donors). **B.** Plot showing mean + SEM of percentages of TNF^+ NK cells per donor of controls (n = 3) and individuals with UC (n = 3). **C.** Representative single and merged fluorescence images of HLA-DP, CD56 and DAPI of control and UC-affected colons. **D.** Fluorescence images of secondary antibody only staining and DAPI. All scale bars: 20 μm.

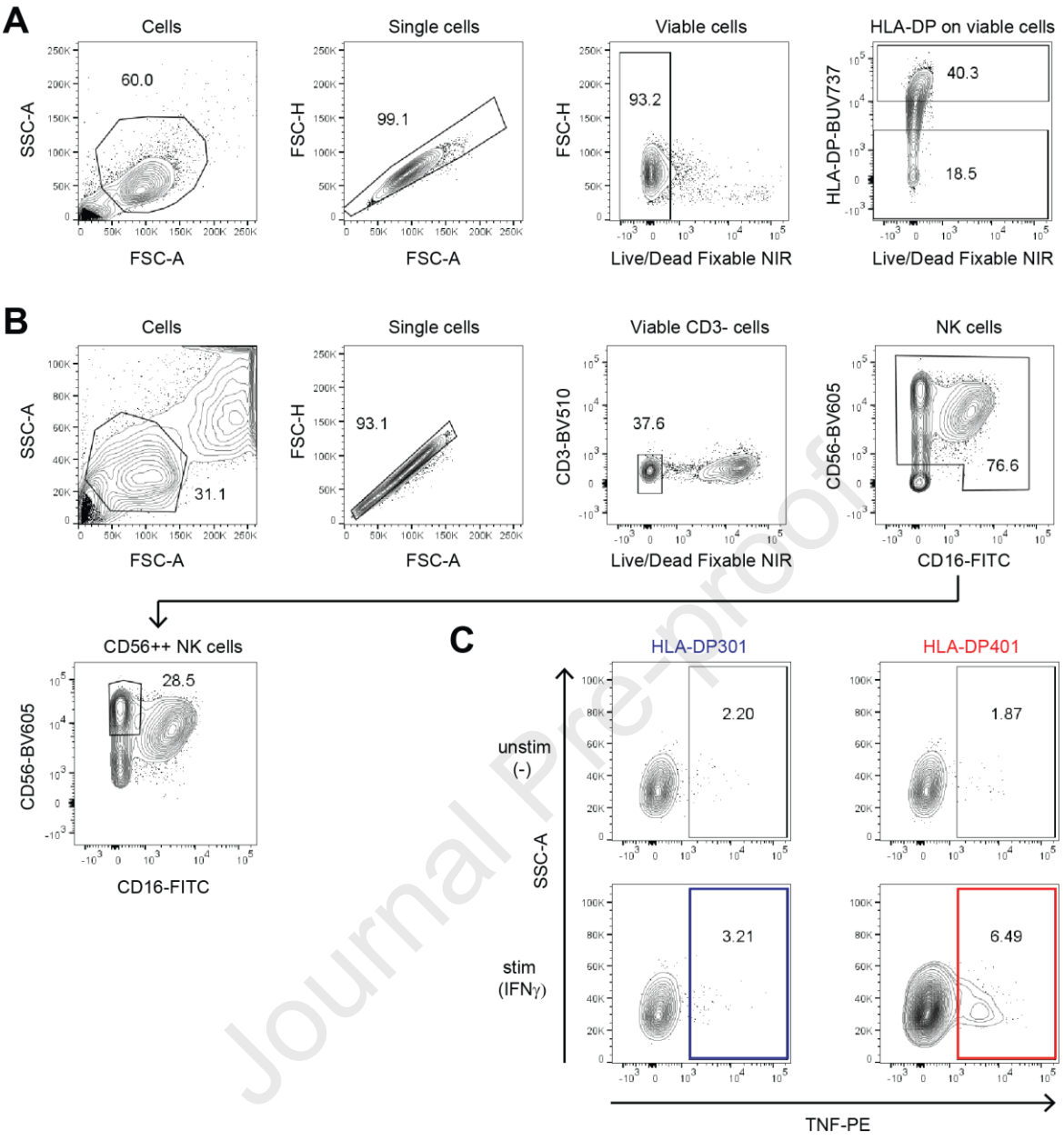

Supplement Figure 7

Supplementary Figure 7: TNF production by CD56^{++} NK cells upon co-culture with HLA-DP401^{+} IECs. A. Gating strategy to identify IECs derived from intestinal organoids for assessment of NKp44 Fc construct binding. IECs are defined as viable cells and were separated into HLA-DP low (lower gate) and high (upper gate) expressing IECs. **B.** Gating

strategy for $CD56^{++}$ NK cells after co-culture with IECs derived from intestinal organoids. $CD56^{++}$ NK cells are defined as single, viable, $CD3^{-}$, $CD16^{-}$, $CD56^{++}$ cells. **C.** Representative flow cytometric plots showing TNF expression of $CD56^{++}$ NK cells after co-culture with HLA-DP301- or HLA-DP401-expressing IECs. IECs were either unstimulated (-) or stimulated (IFNγ) (200 U/ml for 3 days).

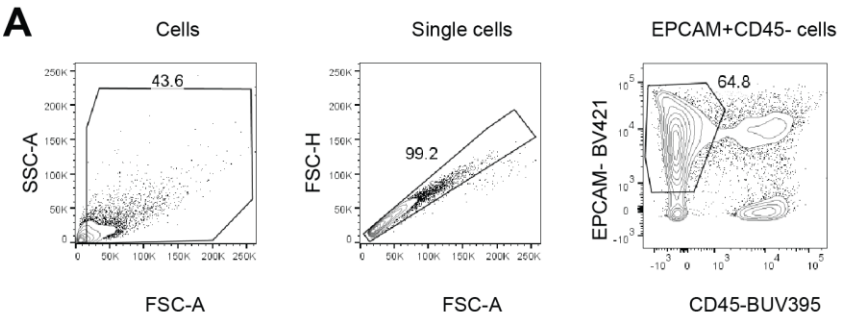

Supplement Figure 8

Supplementary Figure 8: Gating strategies for IECs. A. Gating strategy to identify IECs ($CD45^{-}EpCam^{+}$) derived from intestinal organoids and assess percentage of viable IECs.